

Chapter 3

Single Dish Radio Telescopes

Jayaram N. Chengalur

3.1 Introduction

As a preliminary to describing radio telescopes, it is useful to have a look at the transparency of the atmosphere to electro-magnetic waves of different frequencies. Figure 3.1 is a plot of the height in the atmosphere at which the radiation is attenuated by a factor of 2 as a function of frequency. There are only two bands at which radiation from outerspace can reach the surface of the Earth, one from 3000 \AA to 10000 \AA – the optical/near-infrared window, and one from a few mm to tens of meters – the radio window. Radio waves longer than a few tens of meters get absorbed in the ionosphere, and those shorter than a few mm are strongly absorbed by water vapor. Since mm wave absorption is such a strong function of the amount of water vapour in the air, mm wave telescopes are usually located on high mountains in desert regions.

The optical window extends about a factor of ~ 3 in wavelength, whereas the radio window extends almost a factor of $\sim 10^4$ in wavelength. Hence while all optical telescopes ‘look similar’, radio telescopes at long wavelengths have little resemblance to radio telescopes at short wavelengths. At long wavelengths, radio telescopes usually consist of arrays of resonant structures, like dipole or helical antennas (Figure 3.2). At short wavelengths reflecting telescopes (usually parabolic antennas, which focus incoming energy on to the focus, where it is absorbed by a small feed antenna) are used (Figure 3.3).

Apart from this difference in morphology of antennas, the principal difference between radio and optical telescopes is the use of coherent (i.e. with the preservation of phase information) amplifiers in radio astronomy. The block diagram for a typical single dish radio astronomy telescope is shown in Figure 3.4. Radio waves from the distant cosmic source impinge on the antenna and create a fluctuating voltage at the antenna terminals. This voltage varies at the same frequency as the cosmic electro-magnetic wave, referred to as the **Radio Frequency** (RF). The voltage is first amplified by the front-end (or Radio Frequency) amplifier. The signal is weakest here, and hence it is very important that the amplifier introduce as little noise as possible. Front end amplifiers hence usually use low noise solid state devices, High Electron Mobility Transistors (HEMTs), often cooled to liquid helium temperatures.

After amplification, the signal is passed into a mixer. A mixer is a device that changes the frequency of the input signal. Mixers have two inputs, one for the signal whose frequency is to be changed (the RF signal in this case), the other input is usually a pure sine

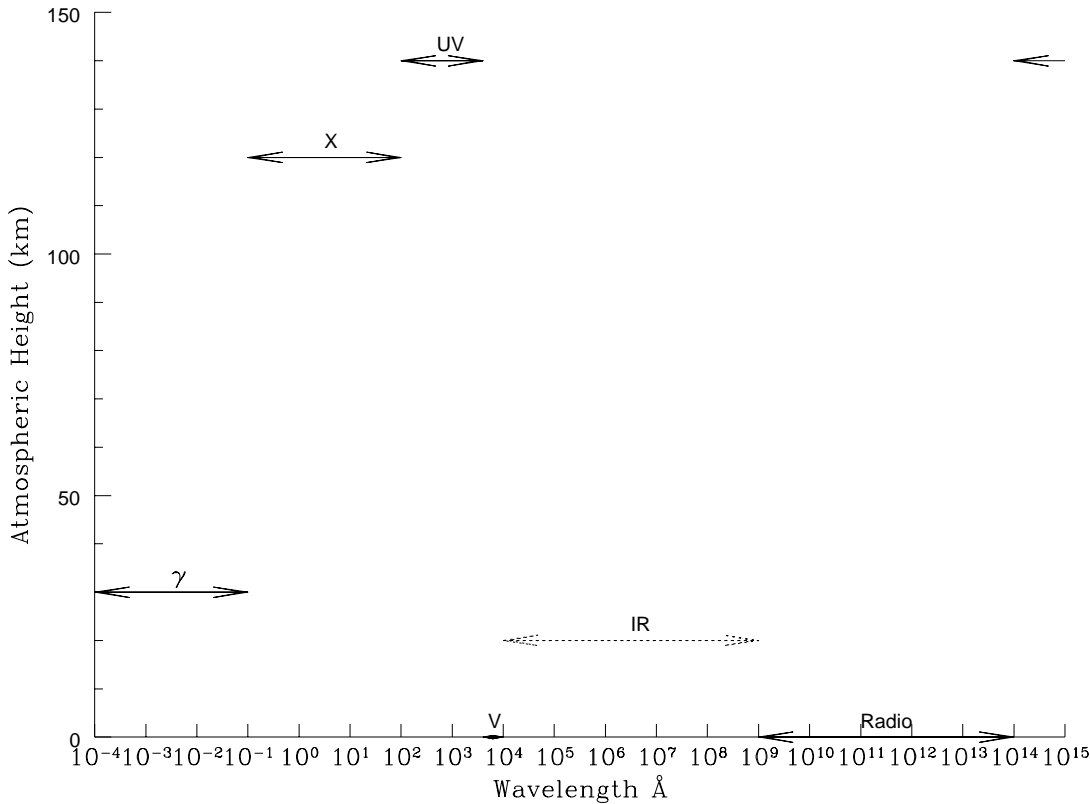


Figure 3.1: The height above the Earth’s surface where cosmic electro-magnetic radiation is attenuated by a factor of two. There are two clear windows the optical (V) ($\sim 4000 - 10000 \text{ \AA}$) and the radio $\sim 1\text{mm} - 10\text{m}$. In addition there are a few narrow windows in the infra-red (IR) wavelength range. At all other wavelengths astronomy is possible only through satellites.

wave generated by a tunable signal generator, the **Local Oscillator (LO)**. The output of the mixer is at the beat frequency of the radio frequency and the local oscillator frequency. So after mixing, the signal is now at a different (and usually lower) frequency than the RF, this frequency is called the **Intermediate Frequency (IF)**. The main reason for mixing (also called heterodyning) is that though most radio telescopes operate at a wide range of radio frequencies, the processing required at each of these frequencies is identical. The economical solution is to convert each of these incoming radio frequencies to a standard IF and then to use the exact same back-end equipment for all possible RF frequencies that the telescope accepts. In telescopes that use co-axial cables to transport the signal across long distances, the IF frequency is also usually chosen so as to minimize transmission loss in the cable. Sometimes there is more than one mixer along the signal path, creating a series of IF frequencies, one of which is optimum for signal transport, another which is optimum for amplification etc. This is called a ‘super-heterodyne’ system. For example, the GMRT (see Chapter 21) accepts radio waves in six bands from 50 MHz to 1.4 GHz and has IFs at 130 MHz, 175 MHz and 70 MHz¹.

¹There are IFs at 130 MHz and 175 MHz to allow the signals from the two different polarizations received



Figure 3.2: The Mauritius Radio Telescope. This is a low frequency (150 MHz) array of which the individual elements are helical antennas.

After conversion to IF, the signal is once again amplified (by the IF amplifier), and then mixed to a frequency range near 0 Hz (the **Base Band** (BB) and then fed into the backend for further specialized processing. What backend is used depends on the nature of the observations. If what you want to measure is simply the total power that the telescope receives then the backend could be a simple square law detector followed by an integrator. (Remember the signal is a *voltage* that is proportional to amplitude of the electric field of the incoming wave, and since the power in the wave goes like the square of its amplitude, the square of the voltage is a measure of the strength of the cosmic source). The integrator merely averages the signal to improve the signal to noise ratio. For spectral line observations the signal is passed into a spectrometer instead of a broad band detector. For pulsar observations the signal is passed into special purpose ‘pulsar machines’. Spectrometers (usually implemented as “correlators”) and pulsar machines are fairly complex and will not be discussed further here (see instead Chapters 8 and 17 for more details). The rest of this chapter discusses only the first part of this block diagram, viz. the antenna itself.

3.2 EM Wave Basics

A cosmic source typically emits radio waves over a wide range of frequencies, but the radio telescope is sensitive to only a narrow band of emission centered on the RF. We can hence, to zeroth order, approximate this narrow band emission as a monochromatic wave. (More realistic approximations are discussed in Chapter 15). The waves leaving the cosmic source have spherical wavefronts which propagate away from the source at the speed of light. Since most sources of interest are very far away from the Earth, the radio telescope only sees a very small part of this spherical wave front, which can be well approximated by a plane wave front. Electro-magnetic waves are vector waves, i.e. the

by the antenna to be frequency division multiplexed onto the same optical fiber for transport to the central electronics building.



Figure 3.3: The Caltech Sub-millimeter Observatory (CSO) at Mauna Kea in Hawaii. The telescope operates in the the sub-mm wavelength range.

electric field has a direction as well as an amplitude. In free space, the electric field of a plane wave is constrained to be perpendicular to its direction of propagation and the power carried by the wave is proportional to the square of the amplitude of the electric field.

Consider a plane EM wave of frequency ν propagating along the Z axis (Figure 3.6). The electric field then can have only two components, one along the X axis, and one along the Y axis. Since the wave is varying with a frequency ν , each of these components also varies with a frequency ν , and at any one point in space the electric field vector will also vary with a frequency ν . The **polarization** of the wave characterizes how the direction of the electric field vector varies at a given point in space as a function of time.

The most general expression for each of the components of the electric field of a plane monochromatic wave² is:

$$E_X = A_X \cos(2\pi\nu t + \delta_X)$$

$$E_Y = A_Y \cos(2\pi\nu t + \delta_Y)$$

where A_X , A_Y , δ_X , δ_Y are constants. If $A_Y = 0$, then the field only has one component along the X axis, which increases in amplitude from $-A_X$ to $+A_X$ and back to $-A_X$ over one period. Such a wave is said to be **linearly polarized** along the X axis. Similarly if A_X is zero then the wave is linearly polarized along the Y axis. Waves which are generated by **dipole** antennas are linearly polarized along the length of the dipole. Now consider a wave for which $A_X = A_Y$, $\delta_X = 0$, and $\delta_Y = -\pi/2$. If we start at a time at which the X component is a maximum, then the Y component is zero and the total field points along the +X axis. A quarter period later, the X component will be zero and the Y component will be at maximum, the total field points along the +Y direction. Another quarter of a period later, the Y component is again zero, and the X component is at minimum, the total field points

²Monochromatic waves are necessarily 100% polarized. As discussed in Chapter 15 quasi-monochromatic waves can be partially polarized.

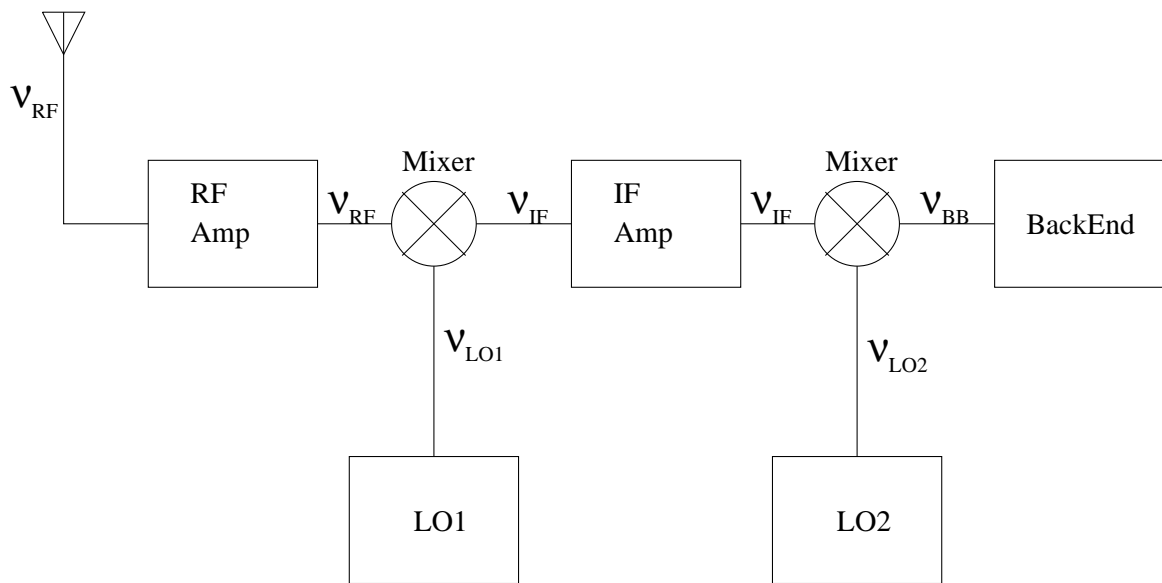


Figure 3.4: Block diagram of a single dish radio telescope.

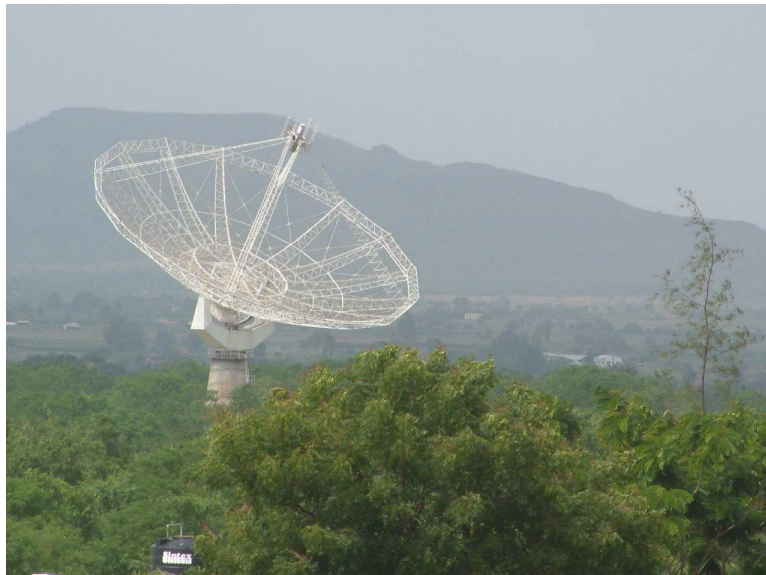


Figure 3.5: One of the 30 GMRT antennas

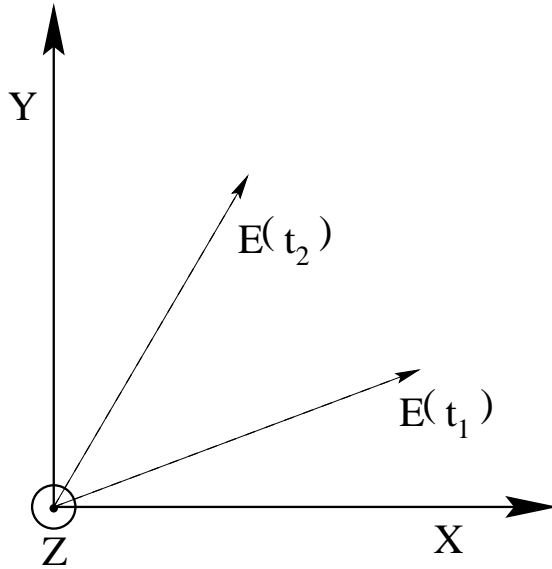


Figure 3.6: Electric field of a plane wave

along the $-X$ direction. Thus over one period, the tip of the electric field vector describes a circle in the XY plane. Such a wave is called **circularly polarized**. If δ_Y were $= \pi/2$ then the electric field vector would still describe a circle in the XY plane, but it would rotate in the opposite direction. The former is called **Right Circular Polarization** (RCP) and the latter **Left Circular Polarization** (LCP).³ Waves generated by **Helical** antennas are circularly polarized. In the general case when all the constants have arbitrary values, the tip of the electric wave describes an ellipse in the XY plane, and the wave is said to be **elliptically polarized**.

Any monochromatic wave can be decomposed into the sum of two orthogonal polarizations. What we did above was to decompose a circularly polarized wave into the sum of two linearly polarized components. One could also decompose a linearly polarized wave into the sum of LCP and RCP waves, with the same amplitude and π radians out of phase. Any antenna is sensitive to only *one* polarization (for example a dipole antenna only absorbs waves with electric field along the axis of the dipole, while a helical antenna will accept only one sense of circular polarization). Note that the reflecting surface of a telescope could well⁴ work for both polarizations, but the feed antenna will respond to only one polarization. To detect both polarizations one need to put two feeds (which could possibly be combined into one *mechanical* structure) at the focus. Each feed will require its own set of electronics like amplifiers and mixers etc.

EM waves are usually described by writing explicitly how the electric field strength varies in space and time. For example, a plane wave of frequency ν and wave number k ($k = 2\pi/\lambda$, $\lambda = c/\nu$) propagating along the Z axis and linearly polarized along the X axis could be described as

$$E(z, t) = A \cos(2\pi\nu t - kz)$$

³This RCP-LCP convention is unfortunately not fixed, and the reverse convention is also occasionally used, leading to endless confusion. It turns out however, that most cosmic sources have very little circular polarization.

⁴Not all reflecting radio telescopes have surfaces that reflect both polarizations. For example, the Ooty radio telescope's (Figure 3.16) reflecting surface consists of a parallel set of thin stainless steel wires, which only reflect the polarization with the electric field parallel to the wires.

This could also be written as

$$E(z, t) = \text{Real}(Ae^{j(2\pi\nu t - kz)})$$

where $\text{Real}()$ implies taking the real part of $()$ and j is the imaginary square root of -1 . Since all the time variation is at the same frequency ν , one could suppress writing it out explicitly and introduce it only when one needs to deal with physical quantities. So, one could equally well describe the wave by the complex quantity \mathbf{A} , where $\mathbf{A} = A e^{-jkz}$, and understand that the physical field is obtained by multiplying \mathbf{A} by $e^{j2\pi\nu t}$ and taking the real part of the product. The field \mathbf{A} is called the **phasor** field⁵. So for example the phasor field of the wave

$$E = A \cos(2\pi\nu t - kz + \delta)$$

is simply $\mathbf{A}e^{j\delta}$.

3.3 Signals and Noise in Radio Astronomy

3.3.1 Signals

At radio frequencies, cosmic source strengths are usually measured in **Janskys**⁶ (**Jy**). Consider a plane wave from a distant point source falling on the Earth. If the energy per unit frequency passing through an area of 1 square meter held perpendicular to the line of sight to the source is 10^{-26} watts then the source is said to have a brightness of 1 Jy, i.e.

$$1 \text{ Jy} = 10^{-26} \text{ W/m}^2/\text{Hz},$$

For an extended source, there is no longer a unique direction to hold the square meter, such sources are hence characterized by a sky brightness B , the energy flow at Earth per unit area, per unit time, per unit solid angle, per unit Frequency, i.e. the units of brightness are $\text{W/m}^2/\text{Hz}/\text{sr}$.

Very often the sky brightness is also measured in temperature units. To motivate these units, consider a black body at temperature T . The radiation from the black body is described by the Planck spectrum

$$B(\nu) = \frac{2h\nu^3}{c^2} \frac{1}{e^{h\nu/kT} - 1} \quad \text{W/m}^2/\text{Hz}/\text{sr}$$

i.e. the same units as the brightness. For a typical radio frequency of 1000 MHz, $h\nu/k = 0.048$, hence

$$e^{h\nu/kT} \sim 1 + h\nu/kT$$

and

$$B(\nu) \simeq \frac{2\nu^2}{c^2} kT = 2kT/\lambda^2$$

This approximation to the Planck spectrum is called the **Rayleigh-Jeans** approximation, and is valid through most of the radio regime. From the R-J approximation,

$$T = \frac{\lambda^2}{2k} B(\nu)$$

⁵For quasi monochromatic waves, (see Chapter 1), one has the related concept of the complex analytical signal

⁶As befitting its relative youth, this is a linear, MKS based scale. At most other wavelengths, the brightness is traditionally measured in units far too idiosyncratic to be described in this footnote.

In analogy, the brightness temperature T_B of an extended source is *defined* as

$$T_B = \frac{\lambda^2}{2k} B(\nu).$$

where $B(\nu)$ is the sky brightness of the source. Note that in general the brightness temperature T_B has no relation to the physical temperature of the source.

For certain sources, like the quiet sun and HII regions, the emission mechanism is **thermal bremsstrahlung**, and for these sources, provided the optical depth is large enough, the observed spectrum will be the Rayleigh-Jeans tail of the black body spectrum. In this case, the brightness temperature is directly related to the physical temperature of the electrons in the source. Sources for which the **synchrotron** emission mechanism dominates, the spectrum is not black-body, but is usually what is called *steep spectrum*⁷, i.e. the flux increases sharply with increasing wavelength. At low frequencies, the most prominent such source is the Galactic non-thermal continuum, for which the flux $S \propto \nu^{-\alpha}$, $\alpha \sim 1$. At low frequencies hence, the sky brightness temperature dominates the system temperature⁸. Pulsars and extended extra-galactic radio sources too in general have steep spectra and are brightest at low frequencies. At the extreme end of the brightness temperature are masers where a lot of energy is pumped out in a narrow collimated molecular line, the brightness temperatures could reach $\sim 10^{12}$ K. This could certainly not be the physical temperature of the source since the molecules disintegrate at temperatures well below 10^{12} K.

3.3.2 Noise

An antenna absorbs power from the radio waves that fall on it. This power is also usually specified in temperature units, i.e. degrees Kelvin. To motivate these units, consider a resistor placed in a thermal bath at a temperature T . The electrons in the resistor undergo random thermal motion, and this random motion causes a current to flow in the resistor. On the average there are as many electrons moving in one direction as in the opposite direction, and the average current is zero. The power in the resistor however depends on the *square* of the current and is not zero. From the equipartition principle one could compute this power as a function of the temperature, and in the radio regime the power per unit frequency is well approximated by the **Nyquist formula**:

$$P = kT,$$

where k is the same Boltzmann constant as in the Planck law. In analogy with this, if a power P (per unit frequency) is available at an antenna's terminals the antenna is *defined* to have an antenna temperature of

$$T_A = \frac{P}{k}$$

Note again that the antenna temperature does not correspond to the physical temperature of the antenna. Similarly the total power available at a radio telescope terminals, referred to the receiver (i.e. the RF amplifier) inputs⁹ is defined as the system temperature T_{sys} , i.e.

$$T_{sys} = \frac{\text{Total Power referred to receiver inputs}}{k}$$

⁷provided that the source is optically thin

⁸See the discussion on system temperature later in this section

⁹By 'referred to the receiver inputs' we mean the following. Suppose you have a noise power P at the output of the radio telescope. If there is only one stage of amplification with gain G , then the power referred to the inputs is P/G . If there is more than one stage of amplification, one has to rescale each noise source along the signal path by the gain of all the preceding amplifiers.

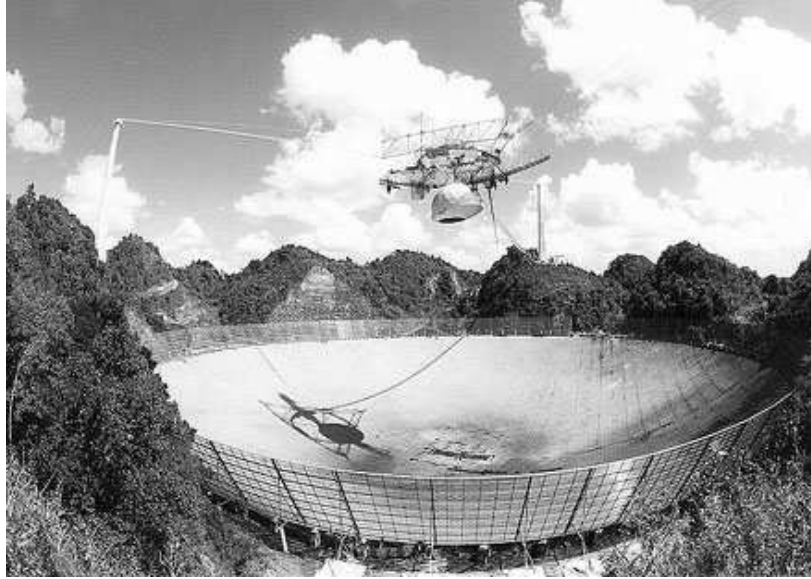


Figure 3.7: The Arecibo telescope consists of a large (300 m) spherical reflector fitted into a naturally occurring valley. The telescope has feeds which are suspended from cables which originate from towers on the surrounding hills. Photo courtesy of NAIC, Arecibo observatory.

The system temperature when looking at blank sky is a measure of the total random noise in the system and hence it is desirable to make the system temperature as low as possible. Noise from the various sub systems that make up the radio telescope are uncorrelated and hence add up linearly. The system temperature can be very generally written as

$$T_{sys} = T_{sky} + T_{spill} + T_{loss} + T_{rec}$$

T_{sky} is the contribution of the background sky brightness. For example the galaxy is a strong emitter of non thermal¹⁰ continuum radiation, which at low frequencies usually dominates the system temperature. At all frequencies the sky contributes at least 3K from the cosmic background radiation.¹¹

The feed antenna is supposed to collect the radiation focused by the reflector. Often the feed antenna also picks up stray radiation from the ground (which radiates approximately like a black body at 300 K) around the edge of the reflector. This added noise is called spillover noise, and is a very important contribution to the system temperature at a telescope like Arecibo. In Figure 3.8 is shown (schematically) the system temperature for the (pre-upgrade) Arecibo telescope at 12cm as a function of the zenith angle at which the telescope is pointed. At high zenith angles the feed radiation spills over the edge of the dish and picks up a lot of radiation from the surrounding hills and the

¹⁰By non thermal radiation one means simply that the source function is not the Planck spectrum.

¹¹Historically, this fact was discovered by Penzias and Wilson when they set out to perform the relatively mundane task of calibrating the system temperature of their radio telescope. This excess 3K discovered to come from the sky was identified with the radiation from the Big Bang, and was one of the powerful pieces of evidence in favour of the Big Bang model. The field of Radio Astronomy itself was started by Karl Jansky, who too was engaged in the task of calibrating the system temperature of his antenna (he had been set the task of characterizing the various kinds of noise which radio receivers picked up, this noise was harmful to trans-atlantic communication, and was hence essential to understand). Jansky discovered that one component of the 'radio noise' was associated with the Galactic center, the first detection of extra-terrestrial radio waves.

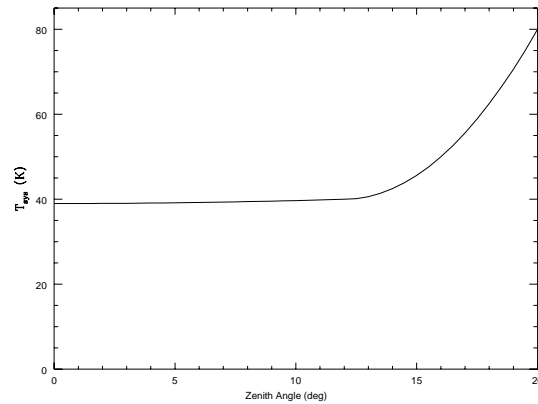


Figure 3.8: Schematic of the variation of T_{sys} with zenith angle for the pre-upgrade Arecibo.

system temperature changes from under 40 K to over 80 K. If a reflecting screen were to be placed around the telescope edges, then, the spill over radiation will be sky radiation reflected by the screen, and not thermal radiation from the ground. At cm wavelengths, $T_{sky} \ll T_{ground}$, so such a ground screen would significantly reduce the system temperature at high zenith angles¹².

Any lossy element in the feed path will also contribute noise (T_{loss}) to the system. This follows from Kirchoff's law which states that good absorbers are also good emitters, and that the ratio of emission to absorption in thermodynamic equilibrium is given by the Planck spectrum at the absorber's physical temperature. This is the reason why there are rarely any uncooled elements between the feed and the first amplifier. Finally, the receiver also adds noise to the system, which is characterized by T_{rec} . The noise added after the first few stages of amplification is usually an insignificant fraction of the signal strength and can often be ignored.

The final, increasingly important contributor to the system temperature is terrestrial interference. If the bandwidth of the interference is large compared to the spectral resolution, the interference is called broad band. Steady, broad band interference increases the system temperature, and provided this increase is small its effects are relatively benign. However, typically interference varies on a very rapid time scale, causing a rapid fluctuation in the system temperature. This is considerably more harmful, since such fluctuations could have harmonics which are mistaken for pulsars etc. In aperture synthesis telescopes such time varying effects will also produce artifacts in the resulting image¹³. Interference whose bandwidth is small compared to the spectral resolution is called narrow band interference. Such interference, provided it is weak enough will corrupt only one spectral channel in the receiver. Provided this spectral channel is not important (i.e. does not coincide with for eg. a spectral line from the source) it can be flagged with little

¹²As can be seen from Figure 3.7, such a screen has indeed been built, and it has dramatically reduced the system temperature at high zenith angles. The wire mesh for this screen was produced, with the co-ordination of NCRA by the same contractor who fabricated the mesh for the GMRT antennas, and was exported to the USA.

¹³It is often claimed that interferometers are immune from interference because different antennas "see" different interfering sources and these do not correlate with one another. However since the interference is typically varying on timescales faster than the system temperature is calibrated, the resulting variations in the system temperatures of the different antennas cause variations in the observed correlation coefficient (for telescopes which do a continuous normalization by the auto-correlation of each antenna's signal) and hence artifacts in the image plane.

loss of information. However, if the interference is strong enough, the receiver saturates, which has several deleterious effects. Firstly since the receiver is no longer in its linear range, the increase in antenna temperature on looking at a cosmic source is no longer simply related to the source brightness, making it difficult, and usually impossible to derive the actual source brightness. This is called **compression**. Further if some other spectral feature is present, perhaps even a spectral line from the source, spurious signals are produced at the beat frequencies of the true spectral line and the interference. These are called **intermodulation products**. Given the increasingly hostile interference environment at low frequencies, it is important to have receivers with large **dynamic range**, i.e. whose region of linear response is as large as possible. It could often be the case, that it is worth increasing the receiver temperature provided that one gains in dynamic range. For particularly strong and steady sources of interference (such as carriers for nearby TV stations), it is usually the practice to block such signals out using narrow band filters before the first amplifier¹⁴.

3.3.3 Signal to Noise Ratio

Since the signals¹⁵ in a radio telescope are random in nature, the output of a total power detector attached to a radio telescope too will show random fluctuations. Supposing a telescope with system temperature T_{sys} , gain G , and bandwidth $\Delta\nu$ is used to try and detect some astrophysical source. The strategy one could follow is to first look at a 'blank' part of the sky, and then switch to a region containing the source. Clearly if the received power increases, then one has detected radio waves from this source¹⁶. But given that the output even on a blank region of sky is fluctuating, how can one be sure that the increase in antenna temperature is not a random fluctuation but is indeed due to the astrophysical source? In order to make this decision, one needs to know what the rms is in the fluctuations. It will be shown later¹⁷, that for a total power detector with instantaneous rms T_{sys} , the rms after integrating a signal of bandwidth $\Delta\nu$ Hz for τ seconds is¹⁸ $T_{\text{sys}}/\sqrt{\Delta\nu\tau}$. The increase in system temperature is just GS , where S is the flux density of the source. The signal to noise ratio is hence

$$\text{snr} = \frac{GS\sqrt{\Delta\nu\tau}}{T_{\text{sys}}}$$

This is the fundamental equation for the sensitivity of a single dish telescope. Provided the signal to noise ratio is sufficiently large, one can be confident of having detected the source.

The signal to noise ratio here considers only the 'thermal noise', i.e. the noise from the receivers, spillover, sky temperature etc. In addition there will be random fluctuations from position to position as discussed below because of confusion. For most single dish radio telescopes, especially at low frequencies, the thermal noise reaches the confusion limit (see Section 3.4) in fairly short integration times. To detect even fainter sources, it becomes necessary then to go for higher resolution, usually attainable only through interferometry.

¹⁴Recall from the discussion above on the effect of introducing lossy elements in the signal path that the price one pays is precisely an increase in receiver temperature

¹⁵Apart from interference etc.

¹⁶Assuming of course that you have enough spatial resolution to make this identification

¹⁷Chapter 5

¹⁸This can be heuristically understood as follows. For a stochastic process of bandwidth $\Delta\nu$, the coherence time is $\sim 1/\Delta\nu$, which means that in a time of τ seconds, one has $\Delta\nu\tau$ independent samples. The rms decreases as the square root of the number of independent samples.

3.4 Antenna Patterns

The most important characteristic of an antenna is its ability to absorb radio waves incident upon it. This is usually described in terms of its effective aperture. The effective aperture of an antenna is defined as

$$A_e = \frac{\text{Power density available at the antenna terminals}}{\text{Flux density of the wave incident on the antenna}}$$

The units are

$$\frac{W/Hz}{W/m^2/Hz} = m^2$$

The effective area is a function of the direction of the incident wave, because the antenna works better in some directions than in others. Hence

$$A_e = A_e(\theta, \phi)$$

This directional property of the antenna is often described in the form of a **power pattern**. The power pattern is simply the effective area normalized to be unity at the maximum, i.e.

$$P(\theta, \phi) = \frac{A_e(\theta, \phi)}{A_e^{max}}$$

The other common way to specify the directive property of an antenna is the **field pattern**. Consider an antenna receiving radio waves from a distant point source. The voltage at the terminals of the antenna as a function of the direction to the point source, normalized to unity at maximum, is called the field pattern $f(\theta, \phi)$ of the antenna. The pattern of an antenna is the same regardless of whether it is used as a transmitting antenna or as a receiving antenna, i.e. if it transmits efficiently in some direction, it will also receive efficiently in that direction. This is called **Reciprocity**, (or occasionally Lorentz Reciprocity) and follows from Maxwell's equations. From reciprocity it follows that the electric field far from a transmitting antenna, normalized to unity at maximum, is simply the Field pattern $f(\theta, \phi)$. Since the power flow is proportional to the square of the electric field, the power pattern is the square of the field pattern. The power pattern is hence real and positive semi-definite.

A typical power pattern is shown in Figure 3.9. The power pattern has a primary maximum, called the **main lobe** and several subsidiary maxima, called *side lobes*. The points at which the main lobe falls to half its central value are called the Half Power points and the angular distance between these points is called the **Half Power Beamwidth (HPBW)**. The minima of the power pattern are called **nulls**. For radio astronomical applications one generally wants the HPBW to be small (so that the nearby sources are not confused with one another), and the sidelobes to be low (to minimize stray radiation). From simple diffraction theory it can be shown that the HPBW of a reflecting telescope is given by

$$\Theta_{HPBW} \sim \lambda/D$$

where D is the physical dimension of the telescope. λ and D must be measured in the same units and Θ is in radians. So the larger the telescope, the better the resolution. For example, the HPBW of a 700 foot telescope at 2380 MHz is about 2 arcmin. This is very poor resolution – an optical telescope ($\lambda \sim 5000\text{\AA}$), a few inches in diameter has a resolution of a few arc seconds. However, the resolution of single dish radio telescopes, unlike optical telescopes, is not limited by atmospheric turbulence. Figure 3.10 shows the power pattern of the (pre-upgrade) Arecibo telescope at 2380 MHz. Although the

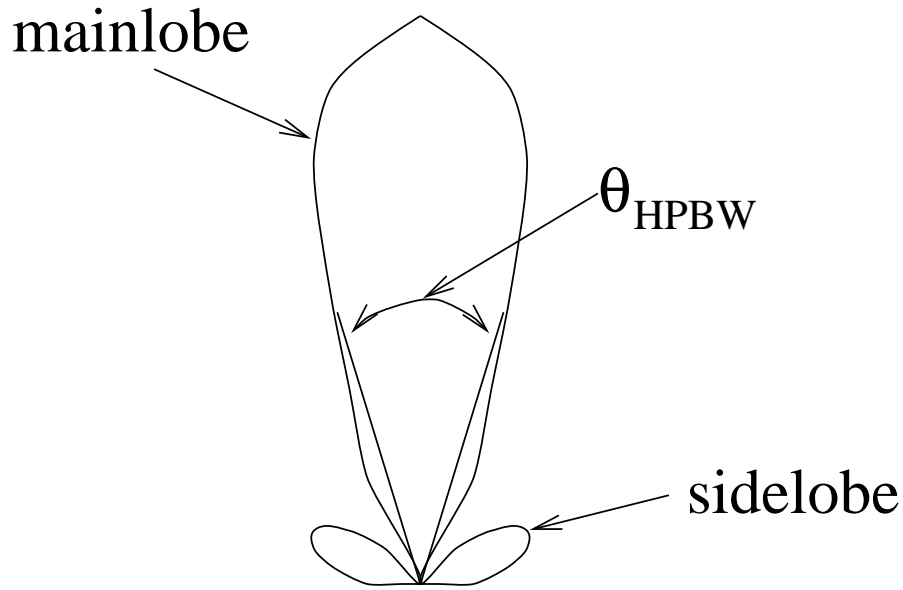


Figure 3.9: Schematic power pattern of an antenna

telescope is 1000 ft in diameter, only a 700 ft diameter aperture is used at any given time, and the HPBW is about 2 arc min. There are two sidelobe rings, which are not quite azimuthally symmetric.

There are two other patterns which are sometimes used to describe antennas. The first is the directivity $D(\theta, \phi)$. The directivity is defined as:

$$D(\theta, \phi) = \frac{\text{Power emitted into } (\theta, \phi)}{(\text{Total power emitted})/4\pi} \quad (3.4.1)$$

$$= \frac{4\pi P(\theta, \phi)}{\int P(\theta, \phi) d\Omega} \quad (3.4.2)$$

$$(3.4.3)$$

This is the ‘transmitting’ pattern of the antenna, and from reciprocity should be the same as the receiving power pattern to within a constant factor. We will shortly work out the value of this constant. The other pattern is the gain $G(\theta, \phi)$. The gain is defined as:

$$G(\theta, \phi) = \frac{\text{Power emitted into } (\theta, \phi)}{(\text{Total power input})/4\pi} \quad (3.4.4)$$

The gain is the same as the directivity, except for an efficiency factor. Finally a figure of merit for reflector antennas is the aperture efficiency, η . The aperture efficiency is defined as:

$$\eta = \frac{A_e^{max}}{A_g} \quad (3.4.5)$$

where A_g is the geometric cross-sectional area of the main reflector. As we shall prove below, the aperture efficiency is at most 1.0.

Consider observing a sky brightness distribution $B(\theta)$ with a telescope with a power pattern like that shown in Figure 3.9. The power available at the antenna terminals is

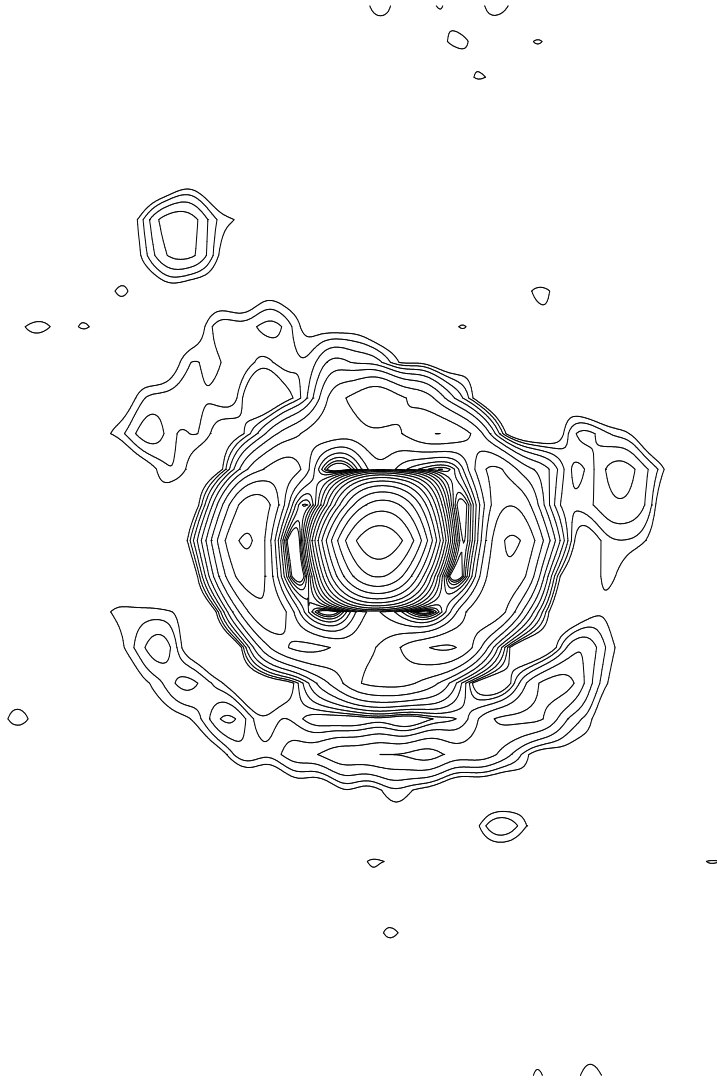


Figure 3.10: The (pre-upgrade) Arecibo power pattern at 2380 MHz. The HPBW is $\sim 2'$.

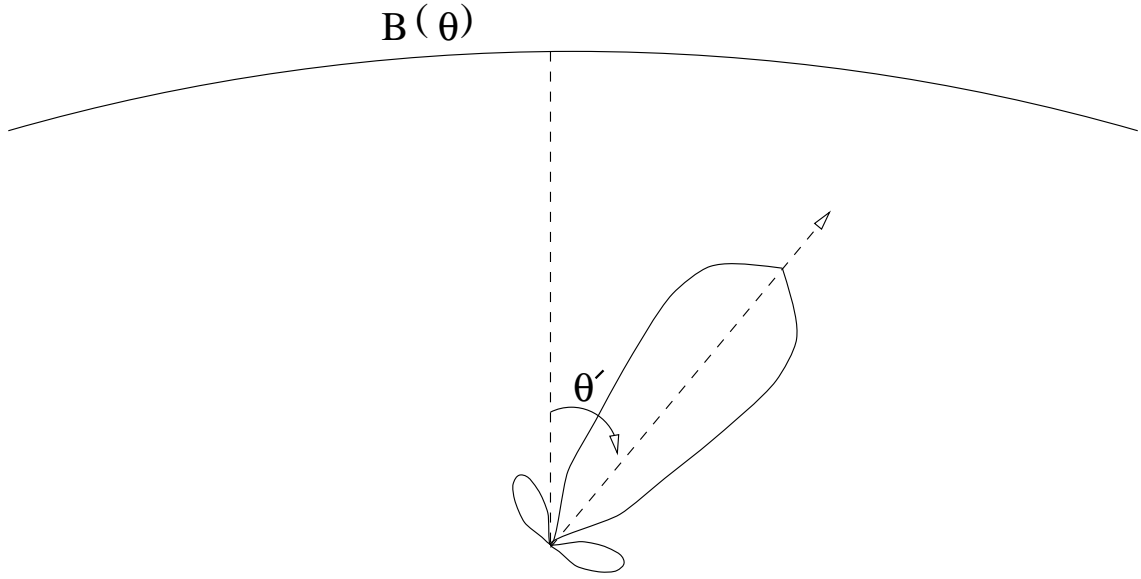


Figure 3.11: The antenna temperature is the convolution of the sky brightness and the telescope beam.

the integral of the brightness in a given direction times the effective area in that direction (Figure 3.11).

$$W(\theta') = \frac{1}{2} \int B(\theta) A_e(\theta - \theta') d\theta \quad (3.4.6)$$

where the available power W is a function of θ' , the direction in which the telescope is pointed. The factor of $\frac{1}{2}$ is to account for the fact that only one polarization is absorbed by the antenna. In two dimensions, the expression for W is:

$$W(\theta', \phi') = \frac{1}{2} \int B(\theta, \phi) A_e(\theta - \theta', \phi - \phi') \sin(\theta) d\theta d\phi \quad (3.4.7)$$

in temperature units, this becomes:

$$T_A(\theta', \phi') = \frac{1}{2} \int \frac{T_B(\theta, \phi)}{\lambda^2} A_e(\theta - \theta', \phi - \phi') \sin(\theta) d\theta d\phi \quad (3.4.8)$$

or

$$T_A(\theta', \phi') = \frac{A_e^{max}}{\lambda^2} \int T_B(\theta, \phi) P(\theta - \theta', \phi - \phi') \sin(\theta) d\theta d\phi \quad (3.4.9)$$

So the antenna temperature is a weighted average of the sky temperature, the weighting function being the power pattern of the antenna. Only if the power pattern is a single infinitely sharp spike is the antenna temperature the same as the sky temperature. For all real telescopes, however, the antenna temperature is a smoothed version of the sky temperature. Supposing that you are making a sky survey for sources. Then a large increase in the antenna temperature could mean either that there is a source in the main beam, or that a collection of faint sources have combined to give a large total power. From the statistics of the distribution of sources in the sky (presuming you know it) and the power pattern, one could compute the probability of the latter event. This gives a lower limit to the weakest detectable source, below this limit, (called the **confusion limit**), one can no longer be confident that increases in the antenna temperature correspond to a

single source in the main beam. The confusion limit is an important parameter of any given telescope, it is a function of the frequency and the assumed distribution of sources.

Now consider an antenna terminated in a resistor, with the entire system being placed in a black box at temperature T . After thermal equilibrium has been reached, the power flowing from the resistor to the antenna is:

$$P_{R \rightarrow A} = kT$$

The power flow from the antenna to the resistor is (from equation (3.4.9) and using the fact that the sky temperature is the same everywhere)

$$P_{A \rightarrow R} = \left(\frac{A_e^{max} kT}{\lambda^2} \right) \int P(\theta, \phi) d\Omega$$

In thermal equilibrium the net power flow has to be zero, hence

$$A_e^{max} = \frac{\lambda^2}{\int P(\theta, \phi) d\Omega}, \quad (3.4.10)$$

i.e. the maximum effective aperture is determined by the *shape* of the power pattern alone. The narrower the power pattern the higher the aperture efficiency. For a reflecting telescope,

$$\int P(\theta, \phi) d\Omega \sim \Theta_{HPBW}^2 \sim \left(\frac{\lambda}{D} \right)^2.$$

so

$$A_e^{max} \sim D^2.$$

The max. effective aperture scales like the geometric area of the reflector, as expected. Also from equation 3.4.10

$$A_e = A_e^{max} P(\theta, \phi) = \frac{\lambda^2 P(\theta, \phi)}{\int P(\theta, \phi) d\Omega}. \quad (3.4.11)$$

Comparing this with equation (3.4.1) gives the constant that relates the effective area to the directivity

$$D(\theta, \phi) = \frac{4\pi}{\lambda^2} A_e(\theta, \phi). \quad (3.4.12)$$

As an application for all these formulae, consider the standard communications problem of sending information from antenna 1 (gain $G_1(\theta, \phi)$, input power P_1) to antenna 2 (directivity $D_2(\theta', \phi')$), at distance R away. What is the power available at the terminals of antenna 2?

The flux density at antenna 2 is given by:

$$S = \frac{P_1}{4\pi R^2} G_1(\theta, \phi)$$

i.e., the power falls off like R^2 , but is not isotropically distributed. (The gain G_1 tells you how collimated the emission from antenna 1 is). The power available at the terminals of antenna 2 is:

$$W = A_{2e} S = \frac{P_1}{4\pi R^2} G_1(\theta, \phi) A_{2e}$$

substituting for the effective aperture from equation (3.4.12)

$$W = \left(\frac{\lambda}{4\pi R} \right)^2 P_1 G_1(\theta, \phi) D_2(\theta', \phi')$$

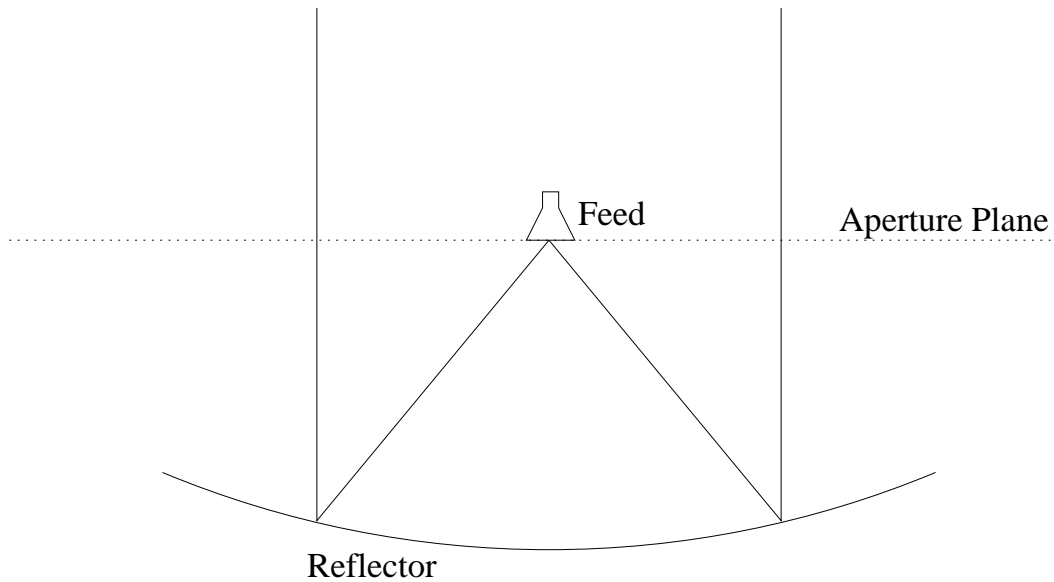


Figure 3.12: Aperture illumination for a parabolic dish.

This is called the **Friis transmission equation**. In Radar astronomy, there is a very similar expression for the power available at an antenna after bouncing off an unresolved target (the **radar range equation**). The major difference is that the signal has to make a round trip, (and the target reradiates power falling on it isotropically), so the received power falls like the fourth power of the distance to the target.

3.5 Computing Antenna Patterns

The next step is to understand how to compute the power pattern of a given telescope. Consider a parabolic reflecting telescope being fed by a feed at the focus. The radiation from the feed reflects off the telescope and is beamed off into space (Figure 3.12). If one knew the radiation pattern of the feed, then from geometric optics (i.e. simple ray tracing, see Chapter 19) one could then calculate the electric field on the plane across the mouth of the telescope (the 'aperture plane'). How does the field very far away from the telescope looklike? If the telescope surface were infinitely large, then the electric field in the aperture plane is simply a plane wave, and since a plane wave remains a plane wave on propagation through free space, the far field is simply a plane wave traveling along the axis of the reflector. The power pattern is an infinitely narrow spike, zero everywhere except along the axis. Real telescopes are however finite in size, and this results in diffraction. The rigorous solution to the diffraction problem is to find the appropriate Green's function for the geometry, this is often impossible in practise and various approximations are necessary. The most commonly used one is Kirchoff's scalar diffraction theory. However, for our purposes, it is more than sufficient to simply use Huygen's principle.

Huygen's principle states that each point in a wave front can be regarded as an imaginary source. The wave at any other point can then be computed by adding together the contributions from each of these point sources. For example consider a one dimensional aperture, of length l with the electric field distribution ('aperture illumination') $e(x)$. The

field at a point $P(R, \theta)$ (Figure 3.13) due to a point source at a distance x from the center of the aperture is (if R is much greater than l) is:

$$dE = \frac{e(x)}{R^2} e^{-j\frac{2\pi x \sin\theta}{\lambda}}$$

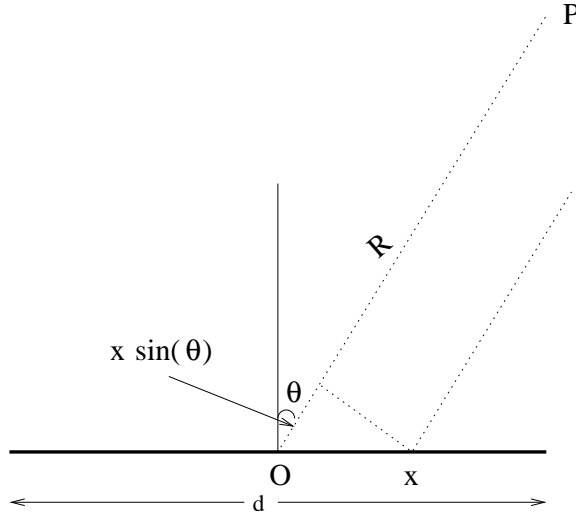


Figure 3.13: The far-field pattern as a function of the aperture illumination.

Where $x \sin \theta$ is simply the difference in path length between the path from the center of the aperture to the point P and the path from point x to point P . Since the wave from point x has a shorter path length, it arrives at point P at an earlier phase. The total electric field at P is:

$$E(R, \theta) = \int_{-l/2}^{l/2} \frac{e(x)}{R^2} e^{-jk\mu x} dx$$

where $k = \frac{2\pi}{\lambda}$ and $\mu = \sin\theta$ and x is now measured in units of wavelength. The shape of the distribution is clearly independent of R , and hence the unnormalized power pattern F_U is just:

$$F_U(\mu) = \int_{-\infty}^{\infty} e_1(x) e^{-jk\mu x} dx \quad (3.5.13)$$

where

$$e_1(x) = e(x) \quad \text{if } |x| \leq l/2 \quad ; \quad 0 \quad \text{otherwise}$$

The region in which the field pattern is no longer dependent on the distance from the antenna is called the **far field region**. The integral operation in equation (3.5.13) is called the **Fourier transform**. $F_U(\mu)$ is the Fourier transform of $e_1(x)$, which is often denoted as $F_U(\mu) = \mathbf{F}[e_1(x)]$. The Fourier transform has many interesting properties, some of which are listed below (see also Section 2.5).

1. Linearity

If $G_1(\mu) = \mathbf{F}[g_1(x)]$ and $G_2(\mu) = \mathbf{F}[g_2(x)]$ then $G_1(\mu) + G_2(\mu) = \mathbf{F}[g_1(x) + g_2(x)]$.

2. Inverse

The Fourier transform is an invertible operation; if

$$G(\mu) = \int_{-\infty}^{\infty} g(x)e^{-j2\pi\mu x} dx$$

then

$$g(x) = \int_{-\infty}^{\infty} G(\mu)e^{j2\pi\mu x} d\mu$$

3. Phase shift

If $G(\mu) = \mathbf{F}[g(x)]$ then $G(\mu - \mu_0) = \mathbf{F}[g(x)e^{-j2\pi\mu_0 x}]$. This means that an antenna beam can be steered across the sky simply by introducing the appropriate linear phase gradient in the aperture illumination.

4. Parseval's theorem

If $G(\mu) = \mathbf{F}[g(x)]$, then

$$\int_{-\infty}^{\infty} |G(\mu)|^2 d\mu = \int_{-\infty}^{\infty} |g(x)|^2 dx$$

This is merely a restatement of power conservation. The LHS is the power outflow from the antenna as measured in the far field region, the RHS is the power outflow from the antenna as measured at the aperture plane.

5. Area

If $G(\mu) = \mathbf{F}[g(x)]$, then

$$G(0) = \int_{-\infty}^{\infty} g(x) dx$$

With this background we are now in a position to determine the maximum effective aperture of a reflecting telescope. For a 2D aperture with aperture illumination $g(x, y)$, from equation (3.4.10)

$$A_e^{max} = \frac{\lambda^2}{\int P(\theta, \phi) d\Omega} = \frac{\lambda^2}{\int |F(\theta, \phi)|^2 d\Omega} \quad (3.5.14)$$

But the field pattern is just the normalized far field electric field strength, i.e.

$$F(\theta, \phi) = \frac{E(\theta, \phi)}{E(0, 0)}$$

where $E(\theta, \phi) = \mathbf{F}[g(x, y)]$. From property (5)

$$E(0, 0) = \int g(x, y) dx dy' \quad (3.5.15)$$

and from Parseval's theorem,

$$\int |E(\theta, \phi)|^2 d\Omega = \int |g(x, y)|^2 dx dy \quad (3.5.16)$$

substituting in equation (3.5.14) using equations (3.5.15), 3.5.16 gives,

$$A_e^{max} = \frac{\lambda^2 \left| \int g(x, y) dx dy \right|^2}{\int |g(x, y)|^2 dx dy}$$

For uniform illumination

$$\frac{A_e^{max}}{\lambda^2} = \frac{A_g^2}{A_g} = A_g$$

Note that since x and y are in units of wavelength, so is A_g . A_e^{max} however is in physical units. Uniform illumination gives the maximum possible aperture efficiency (i.e. 1), because if the illumination is tapered then the entire available aperture is not being used.

As a concrete example, consider a 1D uniformly illuminated aperture of length l . The far field is then

$$\begin{aligned} E(\mu) &= \int_{-l/2}^{l/2} e^{-j2\pi x\mu} dx \\ &= \frac{\lambda \sin(\pi l/\lambda\mu)}{\pi\mu} \end{aligned}$$

and the normalized field pattern is

$$F(\mu) = \frac{\sin(\pi l/\lambda\mu)}{(\pi l/\lambda\mu)}$$

This is called a 1D sinc function. The 1st null is at $\mu = \lambda/l$, the 1st sidelobe is at $\mu = 3/2(\lambda/l)$ and is of strength $2/(3\pi)$. The strength of the power pattern 1st sidelobe is $(2/3\pi)^2 = 4.5\%$. This illustrates two very general properties of Fourier transforms:

1. the width of a function is inversely proportional to width of its transform (so large antennas will have small beams and small antennas will have large beams), and
2. any sharp discontinuities in the function will give rise to sidelobes ('ringing') in the fourier transform.

Figure 3.14 shows a plot of the the power and field patterns for a 700 ft, uniformly illuminated aperture at 2380 MHz.

Aperture illumination design hence involves the following following tradeoffs (see also Chapter 19):

1. A more tapered illumination will have a broader main beam (or equivalently smaller effective aperture) but also lower side lobes than uniform illumination.
2. If the illumination is high towards the edges, then unless there is a very rapid cutoff (which is very difficult to design, and which entails high sidelobes) there will be a lot of spillover.

Another important issue in aperture illumination is the amount of aperture blockage. The feed antenna is usually suspended over the reflecting surface (see Figure 3.3) and blocks out part of the aperture. If the illumination is tapered, then the central part of the aperture has the highest illumination and blocking out this region could have a drastic effect on the power pattern. Consider again a 1D uniformly illuminated aperture of length l with the central portion of length d blocked out. The far field of this aperture is (from the linearity of fourier transforms) just the difference between the far field of an aperture of length l and an aperture of length d , i.e.

$$E(\mu) \propto \frac{\sin(\pi l\mu/\lambda)}{\pi\mu} - \frac{\sin(\pi d\mu/\lambda)}{\pi\mu}$$

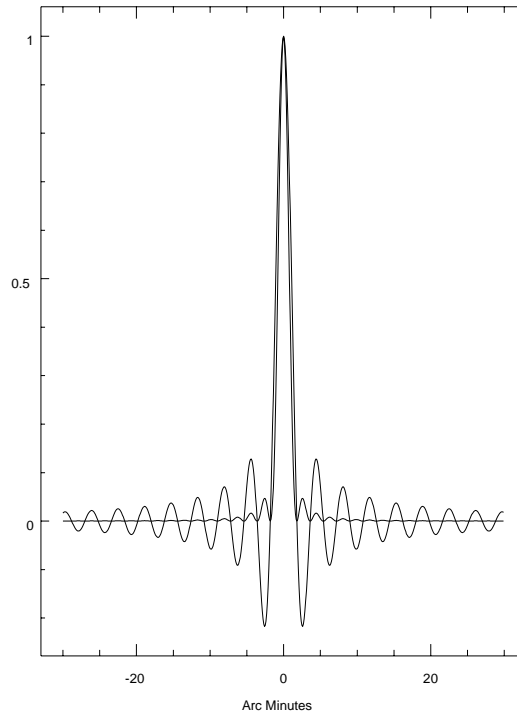


Figure 3.14: Power and field patterns for a 1D uniformly illuminated aperture.

or the normalized field pattern is:

$$F(\mu) = \frac{\lambda}{(l-d)} \left[\frac{\sin(\pi l \mu / \lambda)}{\pi \mu} - \frac{\sin(\pi d \mu / \lambda)}{\pi \mu} \right]$$

The field pattern of the “missing” part of the aperture has a broad main beam (since $d < l$). Subtracting this from the pattern due to the entire aperture will give a resultant pattern with very high sidelobes. In Figure 3.15 the solid curve is the pattern due to the entire aperture, the dotted line is the pattern of the blocked part and the dark curve is the resultant pattern. (This is for a 100ft blockage of a 700 ft aperture at 2380 MHz). Aperture blockage has to be minimized for a ‘clean’ beam, many telescopes have feeds offset from the reflecting surface altogether to eliminate all blockage.

As an example of what we have been discussing, consider the Ooty Radio Telescope (ORT) shown in Figure 3.16. The reflecting surface is a cylindrical paraboloid ($530m \times 30m$) with axis parallel to the Earth’s axis. Tracking in RA is accomplished by rotating the telescope about this axis. Rays falling on the telescope get focused onto the a line focus, where they are absorbed by an array of dipoles. By introducing a linear phase shift across this dipole array, the antenna beam can be steered in declination (the “phase shift” property of Fourier transforms). The reflecting surface is only part of a paraboloid and does not include the axis of symmetry, the feed is hence completely offset, there is no blockage. The beam however is fan shaped, narrow in the RA direction (i.e. that conjugate to the $530m$ dimension) and broad in the DEC (i.e. that conjugate to the $30m$ dimension).

Aperture blockage is one of the reasons why an antenna’s power pattern would deviate from what one would ideally expect. Another common problem that affects the power

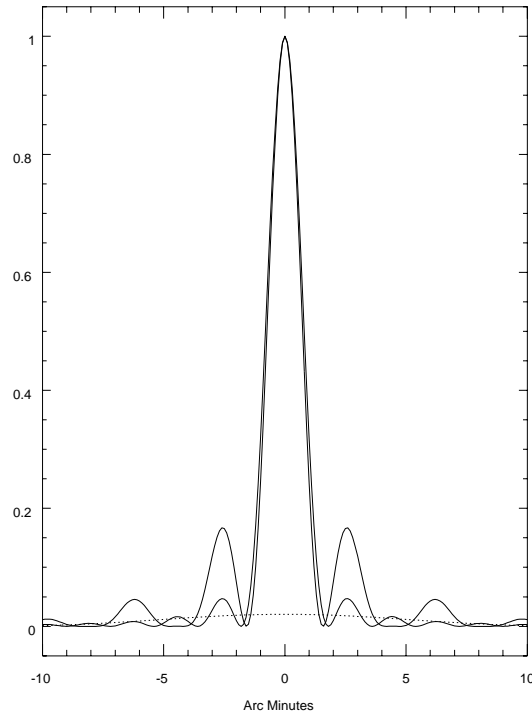


Figure 3.15: Effect of aperture blockage on the power pattern.

pattern is the location of the feed antenna. Ideally the feed should be placed at the focus, but for a variety of reasons, it may actually be displaced from the focus. For example, as the antenna tracks, the reflecting surface gets distorted and/or the feeds legs bend slightly, and for these reasons, the feed is displaced from the actual focal point of the reflector. In an antenna like the GMRT, there are several feeds mounted on a cubic turret at the prime focus, and the desired feed is rotated into position by a servo system (see Chapter 19). Small errors in the servo system could result in the feed pointing not exactly at the vertex of the reflector but along some slightly offset direction. This is illustrated in Figure 3.17. For ease of analysis we have assumed that the feed is held fixed and the reflector as a whole rotates. The solid line shows the desired location of the reflector (i.e. with the feed pointing at its vertex) while the dashed line shows the actual position of the reflector. This displacement between the desired and actual positions of the reflector results in an phase error (produced by the excess path length between the desired and actual reflector positions) in the aperture plane. From the geometry of Figure 3.17 this phase error can be computed, and from it the corresponding distortion in the field and power patterns can be worked out. Figure 3.18[A] shows the result of such a calculation. The principal effect is that the beam is offset slightly, but one can also see that its azimuthal symmetry is lost. Figure 3.18[B] shows the actual measured power pattern for a GMRT antenna with a turret positioning error. As can be seen, the calculated error pattern is a fairly good match to the observed one. Note that in plotting Figure 3.18[B] the offset in the power pattern has been removed (i.e. the power pattern has been measured with respect to its peak position).

Further Reading

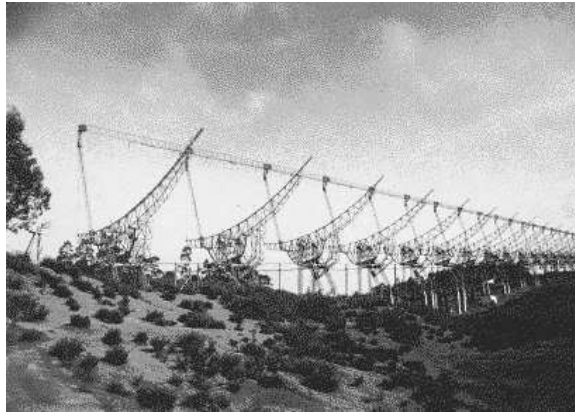
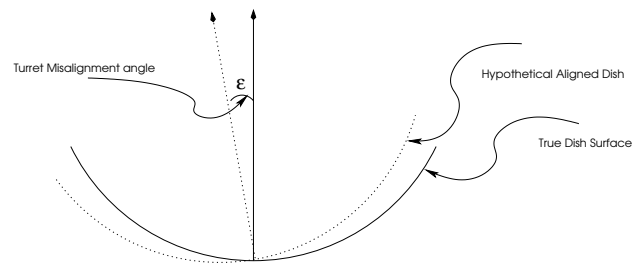
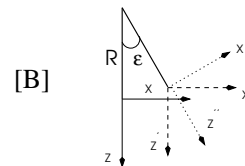


Figure 3.16: The Ooty radio telescope.



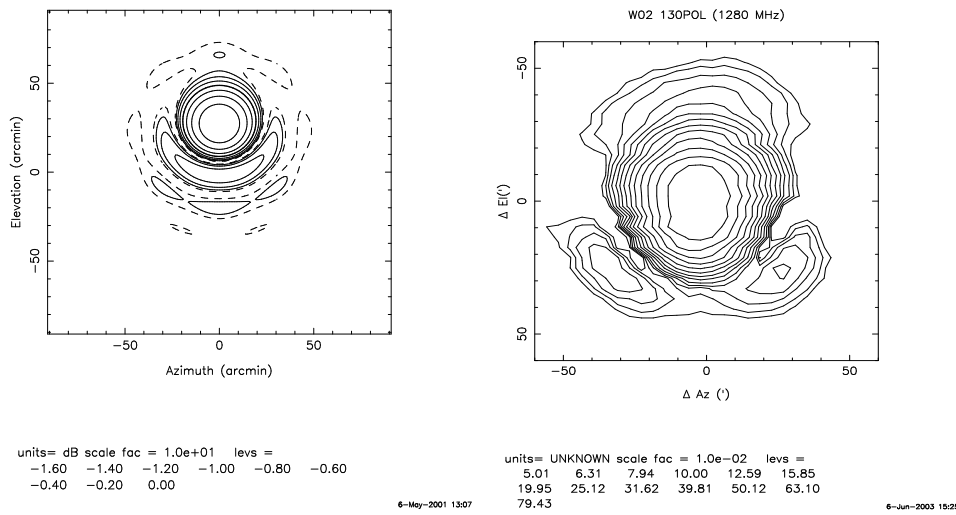
[A]



[B]

Figure 3.17: Turret positioning error. Ideally the feed should point at the vertex of the reflecting surface, but if the feed turret rotation angle is in error then the feed points along some offset direction.

1. Antenna Theory *Analysis and Design* , Constantine A. Balanis, Harper & Row, Publishers, New York.
2. Radio telescopes, *second edition* , W. N. Christiansen & J. A. Hogbom, Cambridge Univ. Press.
3. Microwave Antenna Theory and Design, Samuel Silver (ed.), IEE
4. Reflector Antennas, A. W Love (ed.), IEEE press, *Selected Reprint Series*.
5. Instrumentation and Techniques for Radio Astronomy, Paul F. Goldsmith (ed.), IEEE press *Selected Preprint Series*.



(A)

(B)

Figure 3.18: [A] Calculated beam pattern for a turret positioning error. [B] Measured beam pattern for a turret positioning error. The offset in the pattern has been removed, i.e. the power pattern has been measured with respect to its peak position.